

## Evolution of the electron energy distribution and plasma parameters in a pulsed magnetron discharge

J. T. Gudmundsson, J. Alami, and U. Helmersson

Citation: *Appl. Phys. Lett.* **78**, 3427 (2001); doi: 10.1063/1.1376150

View online: <http://dx.doi.org/10.1063/1.1376150>

View Table of Contents: <http://apl.aip.org/resource/1/APPLAB/v78/i22>

Published by the [AIP Publishing LLC](#).

---

### Additional information on *Appl. Phys. Lett.*

Journal Homepage: <http://apl.aip.org/>

Journal Information: [http://apl.aip.org/about/about\\_the\\_journal](http://apl.aip.org/about/about_the_journal)

Top downloads: [http://apl.aip.org/features/most\\_downloaded](http://apl.aip.org/features/most_downloaded)

Information for Authors: <http://apl.aip.org/authors>



## Evolution of the electron energy distribution and plasma parameters in a pulsed magnetron discharge

J. T. Gudmundsson<sup>a)</sup>

*Science Institute, University of Iceland, Dunhaga 3, IS-107 Reykjavik, Iceland*

J. Alami and U. Helmersson

*Department of Physics, Linköping University, SE-581 83 Linköping, Sweden*

(Received 27 February 2001; accepted for publication 2 April 2001)

We demonstrate the creation of high-density plasma in a pulsed magnetron discharge. A 2.4 MW pulse, 100  $\mu\text{s}$  wide, with a repetition frequency of 50 Hz is applied to a planar magnetron discharge to study the temporal behavior of the plasma parameters: the electron energy distribution function, the electron density, and the average electron energy. The electron density in the vicinity of the substrate, 20 cm below the cathode target, peaks at  $8 \times 10^{17} \text{ m}^{-3}$ , 127  $\mu\text{s}$  after initiating the pulse. Towards the end of the pulse two energy groups of electrons are present with a corresponding peak in average electron energy. With the disappearance of the high-energy electron group, the electron density peaks, and the electron energy distribution appears to be Maxwellian like. Following the electron density peak, the plasma becomes more Druyvesteyn like with a higher average electron energy. © 2001 American Institute of Physics. [DOI: 10.1063/1.1376150]

The dc magnetron sputtering discharge has found widespread use in coating processes, particularly in the deposition of thin metallic films. In magnetron sputter deposition, atoms are sputtered from the cathode target by ions drawn from a magnetically confined plasma. A dense plasma ( $\sim 10^{18} \text{ m}^{-3}$ ) is generally trapped close to the cathode-target surface. However, the plasma densities close to the sample to be deposited ( $\sim 5\text{--}10$  cm below the target) are several orders of magnitude lower ( $10^{15}\text{--}10^{16} \text{ m}^{-3}$ ). Furthermore, the ionized fraction of the sputtered species is small ( $\sim 1\%\text{--}10\%$ ) and the majority of the species extracted on the negatively biased substrates are ions of the discharge gas.

Recently, pulsing the magnetron has been shown to increase the ion density significantly.<sup>1,2</sup> By pulsing the magnetron, very high plasma densities ( $\sim 10^{18} \text{ m}^{-3}$ ) have been obtained 6–10 cm away from the target with a degree of ionization of 30%–70%.<sup>2,3</sup> Furthermore, the target utilization is improved.<sup>1</sup> The pulsed magnetron has been demonstrated for use in high-aspect-ratio filling applications and improved thickness homogeneity of deposited films compared to conventional dc magnetrons.<sup>1</sup> However, the energetics of the discharge, the composition of the plasma, and the reactions among the species remain to be investigated. The fundamental plasma characteristic for better understanding of the plasma chemistry is the electron energy distribution function. Measurements in a conventional dc magnetron indicate that the electron energy distribution on axis is strongly asymmetric, representing a net electron drift from the cathode to the anode.<sup>4</sup> A non-Maxwellian electron energy distribution is to be expected since the source is localized to the magnetic trap region, and at this low neutral pressure (1–5 mTorr) the electron mean-free path is relatively long. The electron energy distribution in a dc argon discharge in the vicinity of the substrate has been measured by Ivanov *et al.*<sup>5</sup> They report

the presence of two energy groups of electrons in the plasma. For sputter deposition of thin films, knowledge of the electron energy distribution and plasma parameters in the near-substrate vicinity are of great importance for determining the process parameters. The aim of this work is to investigate the temporal evolution of the electron energy distribution function (EEDF) and the plasma parameter electron density  $n_e$ , average electron energy  $\langle \mathcal{E} \rangle$ , and plasma potential  $V_{\text{pl}}$  for a pulsed high-density plasma in a magnetron sputtering discharge in the substrate vicinity.

The standard balanced planar magnetron source is operated with a tantalum target of 150 mm diam. The cathode is located inside a stainless-steel sputtering chamber of radius  $R = 60$  cm and height  $L = 75$  cm. Argon of 99.9997% purity is used as the discharge gas. The magnetron cathode was driven by a pulsed power supply that can deliver peak power pulses of up to 2.4 MW (2000 V and 1200 A) at a repetition frequency of 50 Hz and a pulse width in the range of 50–100  $\mu\text{s}$ . For the measurements presented here, the average power was 300 W, pulse width 100  $\mu\text{s}$ , and repetition frequency 50 Hz. The peak voltage was roughly 800 V, and the peak current about 100 A. The argon pressure was 2 mTorr. A cylindrical Langmuir probe, which is a cylindrical tungsten rod of length  $l_{\text{pr}} = 5.5$  mm and radius  $r_{\text{pr}} = 50$   $\mu\text{m}$ , was applied for the measurements. The probe holder is an alumina tube with outer radius  $r_{\text{prh}} = 0.5$  mm and 1.9 cm long. The probe is designed to fulfill the basic requirements for Langmuir-probe diagnostics as discussed by Godyak,<sup>6</sup>  $r_{\text{prh}} \ll l_{\text{pr}}$  and  $r_{\text{pr}}, r_{\text{prh}}, \lambda_{\text{De}} \ll \lambda_e \sim 1$  cm. Here,  $\lambda_{\text{De}} \sim 14\text{--}100$   $\mu\text{m}$  is the Debye length and  $\lambda_e \sim 1$  cm is the electron mean-free path. The probe is positioned perpendicular to the discharge axis, and thus to the electric- and magnetic-field lines 20 cm below the target. The magnetic field at this position is  $< 0.2$  mT, which leads to a gyroradius of  $a_g = (\pi m_e k T_e / 2)^{1/2} / eB \approx 140$   $\mu\text{m}$ , and thus  $r_{\text{pr}} / a_g \approx 0.4$ . Therefore, we can neglect the error in the measured electron density caused by the magnetic field.



after initiating the pulse at 1  $\mu\text{s}$  intervals for a fixed voltage. This was repeated in the voltage range from  $-30$  to  $20$  V at  $0.1$  V intervals. For each time value, the  $I-V$  curve was reconstructed. The measured  $I-V$  curve was smoothed by convoluting a Blackman window to the measured data.<sup>8</sup> The second derivative of the  $I-V$  curve was calculated and the electron energy distribution function  $g_e(\mathcal{E})$  found. The EEDF is given by the Druyvesteyn formula as<sup>9,10</sup>

$$g_e(V) = \frac{2m}{e^2 A_{pr}} \left( \frac{2eV}{m} \right)^{1/2} \frac{d^2 I_e}{dV^2}, \quad (1)$$

where  $\mathcal{E}$  is the electron energy in equivalent voltage units. The plasma potential  $V_{pl}$  is the voltage where the second derivative of the electron current  $I_e$  is zero, and the floating potential  $V_f$  is where the probe draws equal ion and electron currents. The electron density  $n_e$  is determined as

$$n_e = \int_0^\infty g_e(\mathcal{E}) d\mathcal{E}, \quad (2)$$

and the average electron energy  $\langle \mathcal{E} \rangle$  is determined as

$$\langle \mathcal{E} \rangle = \frac{1}{n_e} \int_0^\infty \mathcal{E} g_e(\mathcal{E}) d\mathcal{E}. \quad (3)$$

Figure 1 shows the evolution of the electron energy distribution function with time from initiating the pulse. Initially, the distribution can be described by a single peaked distribution [Fig. 1(a)]. At around 95  $\mu\text{s}$ , a second group of high-energy electrons appears. This high-energy group remains until roughly 115  $\mu\text{s}$  after initiating the pulse. This presence of two energy groups can be seen at 96  $\mu\text{s}$  in Fig. 1(a) and at 105 and 110  $\mu\text{s}$  in Fig. 1(b). At roughly 120  $\mu\text{s}$  after initiating the pulse the electron energy distribution shows a single group of electrons. At roughly 250  $\mu\text{s}$  after initiating the pulse the electron energy distribution reaches the shape that remains for the following 250  $\mu\text{s}$ , as seen in Fig. 1(c). Higher-energy peaks are seen at 350 and 450  $\mu\text{s}$  [Fig. 1(c)]. The evolution of the electron density with time from the initiation of the pulse is shown in Fig. 2(a). The electron density peaks at  $8 \times 10^{17} \text{ m}^{-3}$  127  $\mu\text{s}$  after initiating the pulse. The electron density decreases again and falls to  $8 \times 10^{16} \text{ m}^{-3}$  at 500  $\mu\text{s}$  after initiating the pulse. The measured electron energy distribution function can be fitted to the function

$$g_f(\mathcal{E}) = a \sqrt{\mathcal{E}} \exp(-b\mathcal{E}^x), \quad (4)$$

where  $a$ ,  $b$ , and  $x$  are constants. For  $x=1$ , we have a Maxwellian electron energy distribution, and for  $x=2$  a Druyvesteyn distribution. The value of  $x$  was determined by performing a least-squares analysis of  $\ln[g_f(\mathcal{E})/\sqrt{\mathcal{E}}]$  vs  $\mathcal{E}^x$  for various  $x$  to find the best fit. During the pulse, 50–90  $\mu\text{s}$  after initiating the pulse, the parameter  $x$  is  $\sim 2$ , indicating a Druyvesteyn-like energy distribution. The fitting parameter is  $x \approx 1$  in the range of 115  $\mu\text{s}$ , until 150  $\mu\text{s}$  after initiating the pulse, indicating a Maxwellian-like electron energy distribution. Thus, when the electron density is the most dense,  $3-8 \times 10^{17} \text{ m}^{-3}$ , the electron energy distribution is Maxwellian.

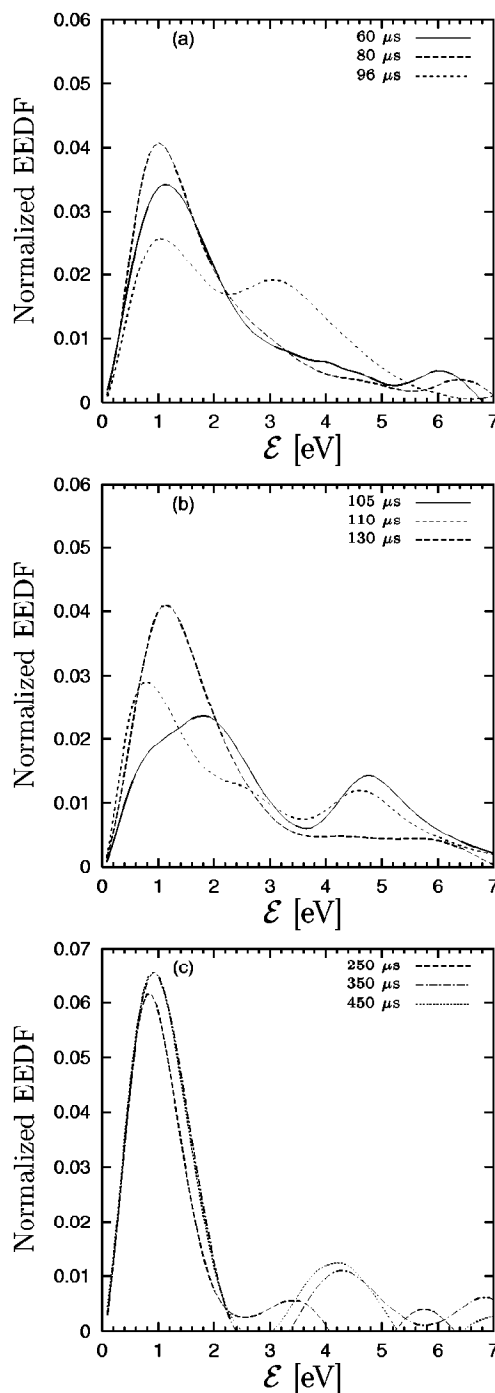


FIG. 1. Normalized EEDF measured (a) during pulses 60, 80, and 100  $\mu\text{s}$  after initiating the pulse; (b) around the electron density maximum 105, 110, and 130  $\mu\text{s}$  after initiating the pulse; and (c) 250, 350, and 450  $\mu\text{s}$  after initiating the pulse. Pulse length, 100  $\mu\text{s}$ ; average power, 300 W; and pressure 2 mTorr.

somewhat overestimated. To correct for this smoothing error, Eq. (4) is fitted to the measured electron energy distribution function from the electron energy where the electron energy distribution function has a maximum value until it has fallen roughly one order of magnitude.<sup>8</sup> The best fit to Eq. (4) is then interpolated to zero electron energy. The interpolated electron energy distribution function is used to extend the

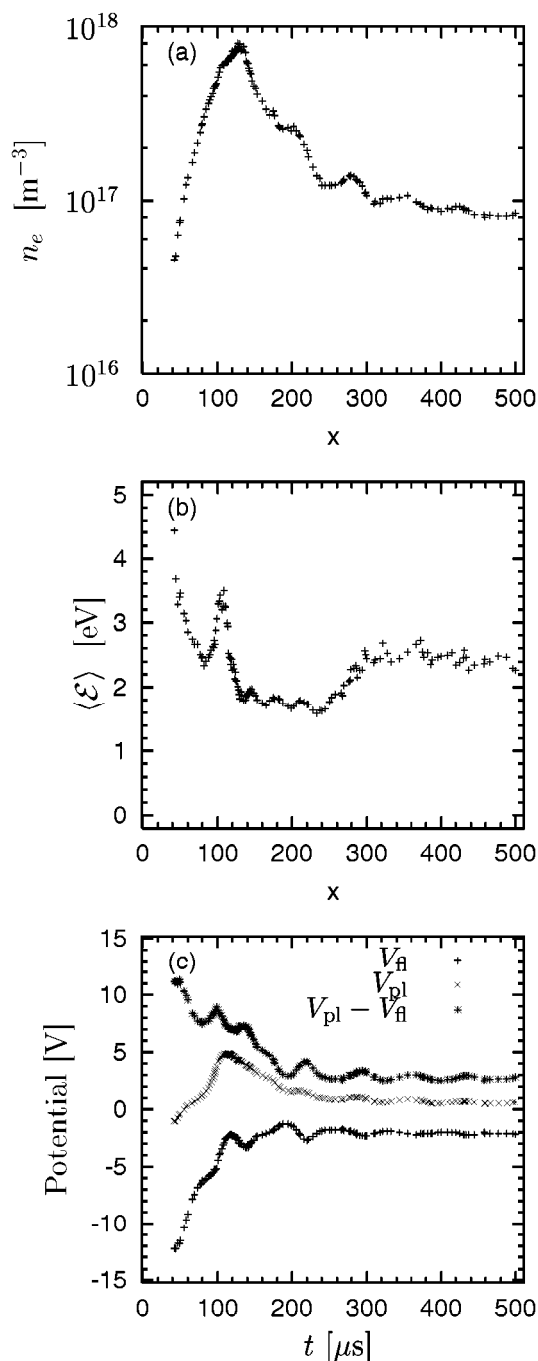


FIG. 2. (a) Electron density, (b) average electron energy, and (c) + floating potential  $V_{fl}$ ,  $\times$  plasma potential  $V_{pl}$ , and \* potential difference ( $V_{pl} - V_{fl}$ ) as a function of time from initiation of the pulse. Target current pulse length, 100  $\mu\text{s}$ ; average power, 300 W; and pressure, 2 mTorr.

electron energy  $\langle \mathcal{E} \rangle$  is shown versus time from initiating the pulse in Fig. 2(b). The average electron energy decreases during the pulse, down to 2.5 eV at 92  $\mu\text{s}$ , where it increases

again with time. The average electron energy peaks at 3.5 eV roughly 100  $\mu\text{s}$  after initiating the pulse. This peak in the average energy coincides with the presence of the high-energy group of electrons apparent in the electron energy distribution. At 127  $\mu\text{s}$ , when the electron density peaks, the average electron energy has decreased to  $\sim 2$  eV. The average electron energy reaches a minimum of about 1.5 eV at 240  $\mu\text{s}$ . It increases again until it reaches a plateau of 2.4 eV at roughly 290  $\mu\text{s}$ , which remains for the following 210  $\mu\text{s}$ . The average electron energy we report in the pulsed magnetron is comparable to what is observed by Sheridan, Goeckner, and Goree.<sup>11</sup> The time evolution of the plasma potential and the floating potential from initiating the pulse is shown in Fig. 2(c). As the energy of ions bombarding a substrate at the floating potential is determined by the difference between the floating potential and the plasma potential ( $V_{pl} - V_{fl}$ ), this value is plotted in Fig. 2(c) as well.

In conclusion, we have measured the temporal behavior of the electron energy distribution function in a pulsed magnetron. Towards the end of the pulse, two energy groups of electrons are present with a corresponding peak in average electron energy. With the disappearance of the high-energy electron group, the electron density peaks, and the electron energy distribution appears to be Maxwellian like. Eventually, the plasma becomes more Druyvesteyn like with lower electron density and higher average electron energy.

This work was partially supported by the Swedish Foundation for Strategic Research and the University of Iceland Research Fund. The company Chemfilt R & D is acknowledged for the use of the power supply.

<sup>1</sup>V. Kouznetsov, K. Macák, J. M. Schneider, U. Helmersson, and I. Petrov, *Surf. Coat. Technol.* **122**, 290 (1999).

<sup>2</sup>K. Macák, V. Kouznetsov, J. M. Schneider, U. Helmersson, and I. Petrov, *J. Vac. Sci. Technol. A* **18**, 1533 (2000).

<sup>3</sup>U. Helmersson, Z. S. Kahn, and J. Alami, in *The Third International Euroconference on Advanced Semiconductor Devices and Microsystems*, Somolenice Castle Slovakia (2000), p. 191, IEEE Catalog No. 00EX386.

<sup>4</sup>T. E. Sheridan, M. J. Goeckner, and J. Goree, *Jpn. J. Appl. Phys., Part 1* **34**, 4977 (1995).

<sup>5</sup>I. Ivanov, S. Statev, V. Orlinov, and R. Shkegov, *Vacuum* **43**, 837 (1992).

<sup>6</sup>V. A. Godyak, in *Plasma-Surface Interactions and Processing of Materials*, edited by O. Auciello (Kluwer Academic, Dordrecht, 1990), pp. 95–134.

<sup>7</sup>E. Passoth, P. Kudrna, C. Csambal, J. F. Behnke, M. Tichú, and V. Helbig, *J. Phys. D* **30**, 1763 (1997).

<sup>8</sup>J. T. Gudmundsson, Memorandum No. UCB/ERL M97/38, Electron Research Laboratory, University of California, Berkeley (1997).

<sup>9</sup>M. J. Druyvesteyn, *Z. Phys.* **64**, 781 (1930).

<sup>10</sup>M. A. Lieberman and A. J. Lichtenberg, *Principles of Plasma Discharges and Materials Processing* (Wiley, New York, 1994).

<sup>11</sup>T. E. Sheridan, M. J. Goeckner, and J. Goree, *J. Vac. Sci. Technol. A* **34**, 2173 (1998).